Localized gap-soliton trains of Bose-Einstein condensates in an optical lattice

D. L. Wang,[1,2,3] X. H. Yan,[1] and W. M. Liu[3]

[1]*College of Science, Nanjing University of Aeronautics and Astronautics, Nanjing 210016, China*
[2]*Department of Physics, Xiangtan University, Xiangtan 411105, China*
[3]*Beijing National Laboratory for Condensed Matter Physics, Institute of Physics,*
Chinese Academy of Sciences, Beijing 100080, China

We develop a systematic analytical approach to study the linear and nonlinear solitary excitations of quasi-one-dimensional Bose-Einstein condensates trapped in an optical lattice. For the linear case, the Bloch wave in the nth energy band is a linear superposition of Mathieu's functions ce_{n-1} and se_n; and the Bloch wave in the nth band gap is a linear superposition of ce_n and se_n. For the nonlinear case, only solitons inside the band gaps are likely to be generated and there are two types of solitons—fundamental solitons (which is a localized and stable state) and subfundamental solitons (which is a localized but unstable state). In addition, we find that the pinning position and the amplitude of the fundamental soliton in the lattice can be controlled by adjusting both the lattice depth and spacing. Our numerical results on fundamental solitons are in quantitative agreement with those of the experimental observation [B. Eiermann *et al.*, Phys. Rev. Lett. **92**, 230401 (2004)]. Furthermore, we predict that a localized gap-soliton train consisting of several fundamental solitons can be realized by increasing the length of the condensate in currently experimental conditions.

PACS number(s): 05.45.Yv, 03.75.Kk, 03.65.Db

I. INTRODUCTION

Loading Bose-Einstein condensates (BECs) in an optical lattice formed by a laser standing wave has received increasing interest in the study of nonlinear atomic optics [1–4]. Understanding the properties of BEC in an optical lattice is of fundamental importance for developing applications of quantum mechanics such as atom lasers and atom interferometers [5–11]. Theoretically, some approximation methods are borrowed from solid state physics, which are used to investigate the dynamics of this system. It is mainly due to the fact that there are considerable resemblances between BEC droplet localized in an optical lattice and electron in a lattice. According to the theory of solid state physics, there exist band gaps between adjacent energy bands in the band structure of the solid. In general, the energy bands exhibits spatially oscillating phenomena. As discussed in Refs. [12,13], however, it is possible to generate soliton in the band gap when the nonlinearity compensates for atom dispersion caused by intersite tunneling. The band gap soliton can be called gap soliton. The existence of the gap solitons was predicted based on coupled-mode theory [14], in analogy to optical gap solitons in Bragg gratings. Such a prediction was validated by a number of groups using some approximation approaches, such as tight binding approximation [12], a complete set of on-site Wannier states [15], an effective mass formula [16], and plane wave method [17]. Although they provide a convenient way to study the gap soliton of the BEC, the validity depends greatly on the nature of the underlying problem. From this point of view, it is desirable to develop a method that does not rely on above approximations [18].

Strictly speaking, an accurate solution can be obtained by exactly solving the full nonlinear Schrödinger equation with a periodic potential. However, it is very difficult to derive analytical solutions because the full nonlinear Schrödinger equation is nonintegrable [19]. Consequently, some asymptotic approaches and numerical simulations are used to investigate this question. Using the multiple scale method, Konotop and Salerno [18] predicted that bright solitons could come into being in a BEC with a positive scattering length and dark solitons could be stable with a negative scattering length. Subsequently, these predictions were proved by using asymptotic theories [20,21]. Employing numerical simulations, Louis *et al.* [22] analyzed the existence and stability of spatially extended (Bloch type) and localized states of a condensate in the band gaps of the linear Bloch-wave spectrum.

Especially, Eiermann *et al.* [23] reported that gap soliton do neither move nor change their shape and atom numbers during propagation. That is to say, the gap soliton is pinned in an optical lattice without attenuation and change in shape. Such a soliton can be regarded as a spatially localized gap soliton, which is also called fundamental soliton in Ref. [24]. More importantly, localized bright solitons would be very useful for future applications, such as atomic interferometry [25]. Subsequently, some explanations to this observation were proposed by using numerical simulations (see Refs. [26–28] and references therein).

To better understand the characteristics of the linear and nonlinear solitary excitations of quasi-one-dimensional (1D) BECs trapped in an optical lattice, we develop a multiple scale method to derive analytically an explicit expression of the wave function. It is found that there are two types of gap solitons in the band gaps. One is the fundamental soliton, which is always stable and pins a fixed position; the other is always unstable and decays gradually due to losing a part of its atoms. The paper is organized as follows: In Sec. II, we derive 1D amplitude and phase equations from the original three-dimensional Gross-Pitaevskii (GP) equation. Subsequently, by analyzing the stability regions of soliton formation, we obtain the formation condition of the fundamental solitons in the band gaps. A linear dispersion relation arising

from the ground state and sound speed of this system in the band gaps are obtained in Sec. III. In Sec. IV, we develop a multiple scale method to study the nonlinear dynamics of the system. We derive a solution of the wave function and discuss its dynamical stability in the band gaps. It is found that the pinning position and amplitude of the fundamental solitons are controlled by adjusting both lattice depth and spacing. Furthermore, we propose an experimental protocol to observe a localized gap train consisting of several fundamental solitons in the condensate under currently experimental conditions. A brief summary is given in Sec. V.

II. EQUATIONS OF AMPLITUDE AND PHASE

Based on mean-field approximation, the time-dependent GP equation of full BEC dynamics reads [17,19,22]

$$i\hbar \frac{\partial \Psi}{\partial T} = \left(-\frac{\hbar^2}{2m}\nabla^2 + V(X,Y,Z) + g|\Psi|^2 \right)\Psi, \quad (1)$$

where $\Psi(X,Y,Z,T)$ is the order parameter of condensate, and (X,Y) and Z are the directions of strong transverse confinement and lattice. $N=\int dr |\Psi|^2$ is the total number of atoms, and $g=4\pi\hbar^2 a_s/m$ is interatomic interaction strength with the atomic mass m and the s-wave scattering length a_s ($a_s>0$ represents the repulsive interaction). The combined potential $V(X,Y,Z)$ of the optical lattice and magnetic trap is

$$V(R^2,Z) = E_0 \sin^2\left(\frac{\pi Z}{d}\right) + \frac{1}{2}m(\omega_\perp^2 R^2 + \omega_Z^2 Z^2),$$

$$\omega_Z \ll \omega_\perp, \quad (2)$$

where $R^2=X^2+Y^2$, E_0 is the lattice depth. $d=\lambda_L/2$ is the lattice spacing, where λ_L is the wavelength of laser beams. ω_Z and $\omega_\perp$ are frequencies of the magnetic trap in the axial (Z) and transverse (X and Y) directions, respectively. By introducing the dimensionless variables $t=\omega_\perp T$, $(r,z)=a_0^{-1}(R,Z)$ with transverse harmonic oscillator length $a_0=\sqrt{\hbar/m\omega_\perp}$, and $\psi=\sqrt{a_0^3/N}\Psi$, we obtain the following dimensionless GP equation:

$$i\frac{\partial \psi}{\partial t} = -\frac{1}{2}\nabla^2\psi + \left[V_0 \sin^2\left(\frac{\pi z}{D}\right) + \frac{1}{2}(r^2 + \Omega^2 z^2) \right]\psi + Q|\psi|^2\psi, \quad (3)$$

where $V_0=E_0/(\hbar\omega_\perp)$, $D=a_0^{-1}d$, $\Omega=\omega_z/\omega_\perp \ll 1$, and $Q=4\pi a_s/a_0$. Expressing the order parameter in terms of modulus and phase, i.e., $\psi=\sqrt{n}\exp(i\Phi)$, and then separating real and imaginary parts, we obtain

$$\frac{\partial n}{\partial t} + \nabla \cdot (n \nabla \Phi) = 0, \quad (4)$$

$$\frac{\partial \Phi}{\partial t} + V_0 \sin^2\left(\frac{\pi z}{D}\right) + \frac{1}{2}(r^2 + \Omega^2 z^2)$$

$$+ \frac{1}{2}(\nabla\Phi)^2 - \frac{1}{2\sqrt{n}}\nabla^2\sqrt{n} + Qn = 0. \quad (5)$$

Equations (4) and (5) are (3+1)-dimensional, nonlinear, and dispersive equations with a variable coefficient. To solve

these equations, we introduce some reasonable approximations. Considering a ^{87}Rb condensate in a cigar-shaped trap with the frequencies of $\omega_z=2\pi\times0.5$ Hz and $\omega_\perp=2\pi\times85$ Hz [23], we obtain $\Omega\approx0.006$. The value of Ω is so small that the variation of the profile of the order parameter is slow in the z direction. Thus, the wave function can be separated by $\psi(r,z,t)=G_0(r)\phi(z,t)$ with $\phi(z,t)=A(z,t)\exp[-i\mu t+i\varphi(z,t)]$. Here, the modulus and the phase are $\sqrt{n}=G_0(r)A(z,t)$ and $\Phi=-\mu t+\varphi(z,t)$, respectively. Owing to the strong confinement in the transverse direction, the spatial structure of function $G_0(r)$ can be well described by a solution of two-dimensional radial symmetric quantum harmonic-oscillator equation, i.e., $\nabla_\perp^2 G_0+2G_0-r^2G_0=0$. The ground-state solution has the form $G_0(r)=C\exp(-r^2/2)$, where $C=1/\sqrt{\pi}$ can be found from the normalization condition $\int_{-\infty}^{\infty}|G_0|^2 r\,dr=1$. Substituting them into Eqs. (4) and (5), we obtain

$$\frac{\partial A}{\partial t} + \frac{\partial A}{\partial z}\frac{\partial \varphi}{\partial z} + \frac{1}{2}A\frac{\partial^2 \varphi}{\partial z^2} = 0, \quad (6)$$

$$-\frac{1}{2}\frac{\partial^2 A}{\partial z^2} + \left[\frac{1}{2}\left(\frac{\partial \varphi}{\partial z}\right)^2 - \mu + 1 + \frac{\partial \varphi}{\partial t} \right.$$

$$\left. + V_0 \sin^2\left(\frac{\pi z}{D}\right) \right]A + Q'A^3 = 0, \quad (7)$$

with $Q'=Q/(2\pi)=2a_s/a_0$. In order to obtain 1D amplitude and phase equations, we have multiplied Eq. (7) by G_0^* and then integrated the resulting equation once with respect to the transverse coordinate to eliminate the dependence on transverse plane. An approach similar to this one has been widely used in quasi-1D (cigar-shaped) BEC problems [22,29,30].

III. LINEAR BLOCH MODES

We now consider a BEC trapped in a 1D optical lattice. Due to the strong confinement in the transverse direction, the system is similar to a waveguide, in which the excitation propagates in the elongated direction [31]. The strong confinement also ensures the dynamical stability of the linear excitation [31]. Therefore, we set $A=u_0(z)+\alpha(z,t)$ with $\alpha(z,t)=\alpha_0 \exp(i\alpha_1)+\text{c.c.}$ and $\varphi=\varphi_0 \exp(i\alpha_1)+\text{c.c.}$ Here, c.c. is complex conjugate and $\alpha_1=kz-\omega t$. k is the wave number and ω is the eigenfrequency. Without loss of generality, we assume $u_0(z)$ characterizing the condensate background. Considering that α_0 and φ_0 are small constants, we obtain

$$i\omega\alpha_0 = ik\varphi_0\frac{\partial u_0}{\partial z} - \frac{1}{2}k^2 u_0\varphi_0, \quad (8)$$

$$(\mu-1)u_0 = -\frac{1}{2}\frac{\partial^2 u_0}{\partial z^2} + V_0\sin^2\left(\frac{\pi z}{D}\right)u_0 + Q'u_0^3, \quad (9)$$
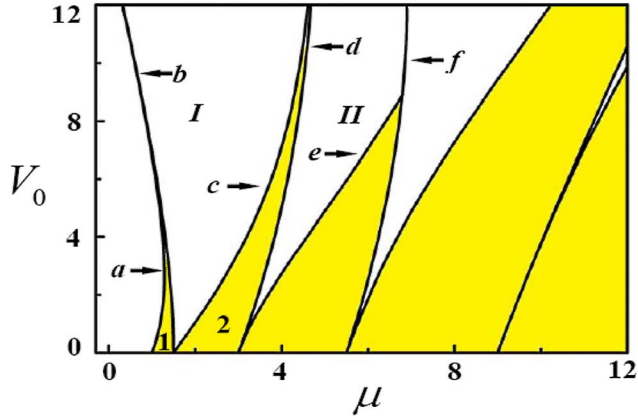
FIG. 1. (Color online). Bloch band of BEC in an optical lattice in the linear regime is functions of the optical depth V_0 and the chemical potential μ. The shaded areas denote the energy bands. The regions 1 and 2 represent the first and second energy band, respectively. The areas I and II represent the lowest two band gaps in the spectrum. Band edges (solid line) $a, b, c, d, e, f, \ldots$ correspond to the eigenvalues and eigenstates $P_0^c(\mathrm{ce}_0)$, $P_1^s(\mathrm{se}_1)$, $P_1^c(\mathrm{ce}_1)$, $P_2^s(\mathrm{se}_2)$, $P_2^c(\mathrm{ce}_2)$, $P_3^s(\mathrm{se}_3), \ldots$ of Mathieu's equation, respectively.

$$(\mu - 1)\alpha_0 = \frac{1}{2}k^2\alpha_0 - i\omega\varphi_0 u_0 + V_0 \sin^2\left(\frac{\pi z}{D}\right)\alpha_0 + 3Q'u_0^2\alpha_0 \tag{10}$$

from the linearization of Eqs. (6) and (7). Under the linear case, $Q' \approx 0$. Equation (9) is turned into Mathieu's equation [32,33]

$$\frac{d^2 u_0}{d\eta^2} + [p + 2q\cos(2\eta)]u_0 = 0, \tag{11}$$

with $\eta = \pi z/D$, $q = -V_0 D^2/(2\pi^2)$, and $p = q + 2D^2(\mu - 1)/\pi^2$. Based on the Floquet-Bloch theorem, u_0 can be represented a superposition of Bloch waves, i.e., $u_0(\eta) = b_1 \exp(i\nu\eta)u_{01}(\eta) + b_2 \exp(-i\nu\eta)u_{02}(\eta)$, where $u_{01}(\eta)$ and $u_{02}(\eta)$ are Mathieu's functions (ce_n or se_n), b_1 and b_2 are arbitrary constants, and ν is a Floquet exponent. If $\cos(\nu\pi) = \pm 1$, the solutions of Mathieu's equation are periodic functions and can be expanded as Fourier series (detailed expression in Ref. [33]).

It should be mentioned that in recent experiments the characteristic lattice spacing d is determined by the angle between the intersecting laser beams forming the lattice and varies in the range $0.4-1.6$ μm [34]. The lattice depth E_0 scales linearly with the light intensity, and varies between 0 and $E_0^{max} \approx 20 E_{rec}$, where $E_{rec} = \pi^2 \hbar^2/(2md^2)$ is the lattice recoil energy [34]. So, the dimensionless parameters V_0 and D are in the range of $0 < V_0 \le 7.0 \times 10^2$ and $0.3 \le D \le 4.05$. For convenience, here we set $D = 3.14$ in our calculation.

From the eigenvalues p and q of Mathieu's function (the textbook analysis can be found, e.g., in Ref. [32]), Fig. 1 presents the band gap diagram for the extended solutions of Eq. (11) which describe noninteracting condensed atoms in an optical lattice. The results are presented for the parameter domain (V_0, μ) relevant to our problem. One can find that the

energy bands (shaded areas) are separated by the band gap regions. In these band gaps, unbounded solutions exist. The band edges correspond to exactly periodic solutions. The regions 1 and 2 represent the first and second energy band, respectively, while the regions I and II denote the first and second band gap, respectively. From Fig. 1, we can conclude that the Bloch wave u_0 in the nth energy band is the linear superposition of the Mathieu's functions ce_{n-1} and se_n, and u_0 in the nth band gap is the linear superposition of ce_n and se_n. As is shown below, a complete band gap spectrum of the matter waves in an optical lattice provides important clues on the existence and the stability regions of solitons.

We next consider the case of $Q' \ne 0$, and discuss the stability problem of soliton formation. Utilizing Eqs. (8)–(10), we obtain

$$\omega^2 = \left(\frac{1}{2u_0}\frac{\partial^2 u_0}{\partial z^2} + \frac{1}{2}k^2 + 2Q'u_0^2\right)\left(\frac{ik}{u_0}\frac{\partial u_0}{\partial z} + \frac{1}{2}k^2\right). \tag{12}$$

Setting $\omega = \omega_r + i\omega_i$ (where the subscripts denote the real and imaginary parts) [35], one obtains

$$\omega_r^2 = (\gamma/4)\sqrt{k^4 + (4k^2/u_0^2)\left(\frac{\partial u_0}{\partial z}\right)^2} + (k^2\gamma/4)$$

and

$$\omega_i^2 = (\gamma/4)\sqrt{k^4 + (4k^2/u_0^2)\left(\frac{\partial u_0}{\partial z}\right)^2} - (k^2\gamma/4),$$

where

$$\gamma = [1/(2u_0)]\frac{\partial^2 u_0}{\partial z^2} + k^2/2 + 2Q'u_0^2$$

If the imaginary part of quasiparticle frequency is a nonzero value, the corresponding Bloch wave exhibits exponential growth and hence the state ψ is dynamical instability [22]. If the frequency of the associated quasiparticle spectrum is real, the soliton would be stable. From the expression of the imaginary part of the frequency, one can see the dependence of the instability growth rate ω_i on k and $\frac{1}{u_0}\frac{\partial u_0}{\partial z}$. On the one hand, when $k = 0$, one finds $\omega = 0$, which is an inessential solution. On the other hand, it is impossible for $\frac{1}{u_0}\frac{\partial u_0}{\partial z}$ being equal to zero because u_0 is the Bloch wave in the energy bands or band gaps. If $\frac{1}{u_0}\frac{\partial u_0}{\partial z}$ is a purely imaginary number [also obtained from Eq. (12)], the wave function ψ possesses dynamical stability. We therefore conclude that the stable condition of soliton formation is $u_0 = \exp(i\beta z)$, where β is an arbitrary real constant. Because the Bloch wave in the nth energy band is the linear superposition of the Mathieu's functions ce_{n-1} and se_n, it does not satisfy the stable condition. Only if Bloch wave in the nth band gap has the form of $u_0 = \beta \mathrm{ce}_n + \beta i \, \mathrm{se}_n$, the soliton possesses dynamical stability. Thus the linear dispersion relation of the nth band gap is

$$\omega^2 = \left(\frac{k^2}{2} - \frac{kn\pi}{D}\right)\left(\frac{k^2}{2} - \frac{n^2\pi^2}{2D^2} + 2Q'u_0^2\right). \tag{13}$$

Under long-wave approximation, the sound speed is

$$V_g = \lim_{k \to 0} \frac{\partial \omega}{\partial k} = \pm \sqrt{Q' u_0^2 - \frac{n^2}{4} \left(\frac{\pi}{D} \right)^2}, \qquad (14)$$

where the positive (negative) sign represents the rightward (leftward) propagation of the wave packets. For the case of $D \to \infty$, the external potential would be a harmonic potential [see Eq. (2)] and a corresponding sound speed is $V_{gh} = \sqrt{Q'} u_0$ in our notation. This behavior is consistent with both the experimental [36] and theoretical results [30]. Obviously, the second term under the radical sign in Eq. (14) is arisen from the optical lattice potential. The sound speed is the largest in the first band gap and gradually decreases with n. Generally speaking, the value of $1/D$ in the experiments [23,34] would be larger than that of Q'. It implies that the linear dispersion relation and sound speed are dependent mainly on the lattice spacing.

IV. NONLINEAR BLOCH MODES

A. The explicit expression of the wave function

To better understand the nonlinear dynamics of BEC in an optical lattice, we here develop a multiple scale method to derive an explicit expression of the wave function of the condensates in an optical lattice. By means of asymptotic expansion in nonlinear perturbation theory, we propose that the amplitude and phase can be expanded by multiple scale methods. In the case of that, mathematically, any parameter can be defined as a function of fast and slow variables, we propose each order parameter of the amplitude and phase can be written to a function of a fast and two slow variables. That is to say, the amplitude and phase of the wave function are sought for the forms of $A = u_0(z_0, \xi, \tau) + \varepsilon[a^{(0)}(z_0, \xi, \tau) + \varepsilon^2 a^{(1)}(z_0, \xi, \tau) + \cdots]$ and $\varphi = \varepsilon^2[\varphi^{(0)}(z_0, \xi, \tau) + \varepsilon^2 \varphi^{(1)}(z_0, \xi, \tau) + \cdots]$, respectively, where the small parameter ε represents the relative amplitude of extended states in BEC. Slow variables $\xi = \varepsilon(z - V_g t)$ and $\tau = \varepsilon^3 t$ characterize the slow variation of soliton dynamics. Fast variable $z_0 = z$ denotes the propagation direction of the lattice wave packets. V_g is a group velocity. By substituting them into Eqs. (6) and (7), and then separating them in terms of ε, Eq. (6) can be written as

$$V_g \frac{\partial u_0}{\partial \xi} = 0, \qquad (15)$$

$$V_g \frac{\partial a^{(0)}}{\partial \xi} = \frac{\partial u_0}{\partial z_0} \frac{\partial \varphi^{(0)}}{\partial z_0} + \frac{1}{2} u_0 \frac{\partial^2 \varphi^{(0)}}{\partial z_0^2}, \qquad (16)$$

$$\frac{\partial u_0}{\partial z_0} \frac{\partial \varphi^{(0)}}{\partial \xi} + \frac{\partial u_0}{\partial \xi} \frac{\partial \varphi^{(0)}}{\partial z_0} + \frac{\partial a^{(0)}}{\partial z_0} \frac{\partial \varphi^{(0)}}{\partial z_0} = -\frac{\partial u_0}{\partial \tau}, \qquad (17)$$

$$V_g \frac{\partial a^{(1)}}{\partial \xi} = \frac{\partial a^{(0)}}{\partial \tau} + \frac{\partial a^{(0)}}{\partial \xi} \frac{\partial \varphi^{(0)}}{\partial z_0} + \frac{1}{2} u_0 \frac{\partial^2 \varphi^{(0)}}{\partial \xi^2} + \frac{1}{2} u_0 \frac{\partial^2 \varphi^{(1)}}{\partial z_0^2}$$
$$+ a^{(0)} \frac{\partial^2 \varphi^{(0)}}{\partial z_0 \partial \xi} + \frac{\partial u_0}{\partial z_0} \frac{\partial \varphi^{(1)}}{\partial z_0} + \frac{\partial u_0}{\partial \xi} \frac{\partial \varphi^{(0)}}{\partial \xi} + \frac{\partial a^{(0)}}{\partial z_0} \frac{\partial \varphi^{(0)}}{\partial \xi}. \qquad (18)$$

Equation (7) becomes

$$-\frac{1}{2} \frac{\partial^2 u_0}{\partial z_0^2} - (\mu - 1) u_0 + V_0 \sin^2 \left(\frac{\pi z_0}{D} \right) u_0 + Q' u_0^3 = 0, \qquad (19)$$

$$-\frac{1}{2} \frac{\partial^2 a^{(0)}}{\partial z_0^2} - (\mu - 1) a^{(0)} + V_0 \sin^2 \left(\frac{\pi z_0}{D} \right) a^{(0)} + 3 Q' u_0^2 a^{(0)}$$
$$= \frac{\partial^2 u_0}{\partial z_0 \partial \xi}, \qquad (20)$$

$$-\frac{\partial^2 a^{(0)}}{\partial z_0 \partial \xi} + 3 Q' u_0 (a^{(0)})^2 = \frac{1}{2} \frac{\partial^2 u_0}{\partial \xi^2}, \qquad (21)$$

$$-\frac{1}{2} \frac{\partial^2 a^{(1)}}{\partial z_0^2} - (\mu - 1) a^{(1)} + V_0 \sin^2 \left(\frac{\pi z_0}{D} \right) a^{(1)} + 3 Q' u_0^2 a^{(1)}$$
$$= \frac{1}{2} \frac{\partial^2 a^{(0)}}{\partial \xi^2}, \qquad (22)$$

$$\frac{\partial^2 a^{(1)}}{\partial z_0 \partial \xi} - 6 Q' u_0 a^{(0)} a^{(1)} = \frac{1}{2} u_0 \left(\frac{\partial \varphi^{(0)}}{\partial z_0} \right)^2 - V_g a^{(0)} \frac{\partial \varphi^{(0)}}{\partial \xi}. \qquad (23)$$

From Eq. (15), one can see that u_0 is independent on ξ. Due to the fast and slow varies possess different physical connotation, so it is reasonable that these order parameters are written to arithmetic multiply of function of the fast and slow variables. We may set $u_0(z_0, \tau) = u_{01}(z_0) u_{03}(\tau)$. Similarly, $a^{(i)}$ and $\varphi^{(i)}$ are the forms of $a^{(i)}(z_0, \xi, \tau) = a_{i1}(z_0) a_{i2}(\xi) a_{i3}(\tau)$ and $\varphi^{(i)}(z_0, \xi, \tau) = \varphi_{i1}(z_0) \varphi_{i2}(\xi) \varphi_{i3}(\tau)$, respectively, where $i = 0, 1, 2, \ldots$. Note that the form of Eq. (19) is the same as that of Eq. (9). In view of the fact that BEC in the experiments are dilute and weakly interacting: $n |a_s|^3 \ll 1$, where n is the average density of the condensate, so Eq. (19) can also be transformed into Mathieu's equation under the consideration of weak nonlinearity. The solutions of Mathieu's equation have been discussed in Sec. III. By comparing Eq. (19) with Eq. (20), one finds $a^{(0)} = 0$. From Eq. (16), we obtain $u_0 = (\frac{\partial \varphi^{(0)}}{\partial z_0})^{-(1/2)}$. So, Eq. (17) becomes

$$-\frac{\frac{\partial \varphi_{03}}{\partial \tau}}{\varphi_{03}^2} = \frac{\frac{\partial^2 \varphi_{01}}{\partial z_0^2} \varphi_{01} \frac{\partial \varphi_{02}}{\partial \xi}}{\frac{\partial \varphi_{01}}{\partial z_0}}. \qquad (24)$$

The left-hand side of Eq. (24) is the differentiation of φ_{03} with respect to τ, while the right-hand side of Eq. (24) is differentiation of φ_{01} (φ_{02}) with respect to z_0 (ξ). Obviously, both sides of the equation must be equal to a constant λ, i.e., $\varphi_{03} = 1/(\lambda \tau)$, and $\varphi_{02} = -(1/2) \lambda u_{01} \xi [\frac{\partial u_{01}}{\partial z_0} \int \frac{dz_0}{[u_{01}(z_0)]^2}]^{-1}$. So, $\varphi^{(0)} = -[u_{01} \xi/(2\tau)][\frac{\partial u_{01}}{\partial z_0}]^{-1}$. Correspondingly, we obtain

$$\frac{\partial u_{03}(\tau)}{\partial \tau} = \frac{u_{03}(\tau)}{2\tau}. \qquad (25)$$

Similarly, from Eqs. (18), (22), and (23), we have

$$a^{(1)} = \frac{u_0 \xi^3}{24\tau^2 \left[\frac{\partial^2 u_0}{\partial z_0^2} + 4Q' u_0^3 \right]} \frac{\partial}{\partial z_0} \left\{ u_0 \left[1 - u_0 \frac{\partial^2 u_0}{\partial z_0^2} \left(\frac{\partial u_0}{\partial z_0} \right)^{-2} \right]^2 \right\}.$$

(26)

Under the transformations $z_0 = z$, $\xi = \varepsilon(z - V_g t)$, and $\tau = \varepsilon^3 t$, the perturbation parameters can be written as $u_0(z,t) = u_{01}(z)\sqrt{t}$, $\varepsilon^2 \varphi^{(0)} = -[(z - V_g t)u_0/(2t)][\frac{\partial u_0}{\partial z}]^{-1}$, and $\varepsilon^3 a^{(1)} = \{u_0(z - V_g t)^3/[24t^2(\frac{\partial^2 u_0}{\partial z^2} + 4Q' u_0^3)]\}\frac{\partial}{\partial z}\{u_0[1 - u_0\frac{\partial^2 u_0}{\partial z^2}(\frac{\partial u_0}{\partial z})^{-2}]^2\}$, where $u_{01}(z)$ is the nonlinear Bloch wave of BEC in an optical lattice. Finally, the solution of the dimensionless GP equation (3) is given by

$$\psi(r,z,t) = \sqrt{\frac{1}{\pi}} \exp\left(-\frac{r^2}{2} \right) \left(u_{01} + \frac{u_{01}(z - V_g t)^3}{24t^2 \left[\frac{\partial^2 u_{01}}{\partial z^2} + 4tQ' u_{01}^3 \right]} \right.$$
$$\times \frac{\partial}{\partial z} \left\{ u_{01} \left[1 - u_{01} \frac{\partial^2 u_{01}}{\partial z^2} \left(\frac{\partial u_{01}}{\partial z} \right)^{-2} \right]^2 \right\} \right)$$
$$\times \exp\left[-i\mu t - i\frac{(z - V_g t)u_{01}}{2t} \left(\frac{\partial u_{01}}{\partial z} \right)^{-1} \right], \quad (27)$$

where the Bloch waves u_{01} and group velocity V_g can be given in Sec. III. μ is the chemical potential. Equation (27) is just an explicit expression of the wave function for 1D BEC trapped in an optical lattice.

As is discussed in Sec. III, the Bloch wave in the nth energy band is the linear superposition of the Mathieu's functions ce_{n-1} and se_n, which does not satisfy the stable condition of soliton formation. Therefore, the condensate in the energy band region cannot generate soliton, only the condensates in the band gaps may occur in the soliton. In the following we discuss soliton dynamical stabilities of the condensates in the band gaps. The stability of soliton in nonlinear systems is an important issue, since only dynamically stable modes are likely to be generated and observed in experiments.

B. Soliton properties in the band gaps

To link our analytical results to real experiments, we estimate the values of the dimensionless parameters in Eq. (27) according to actual physical quantities. We consider a cigar-shaped ^{87}Rb condensate (atomic mass 1.4×10^{-25} kg and the scattering length 5.3 nm) containing $N = 900$ atoms in a trap with $\omega_z = 2\pi \times 0.5$ Hz and $\omega_\perp = 2\pi \times 85$ Hz (The data are from the experiment [23]). The parameter $\Omega \approx 0.006 \ll 1$ in Eq. (3). It implies that the condensate may be regarded as a quasi-1D optical lattice in the direction of a weak confinement. Hereafter the radial radius is determined by $r = 0.01$. Based on that 1D optical lattice is created from one pair of counterpropagating laser beams in real experiments, the lattice depth and the lattice spacing depend on the peak intensity and the angle of the two identical counterpropagating laser beams, respectively. For the wavelength $\lambda_L = 783$ nm, used in Ref. [23], this angle between counterpropagating laser beams would be equal to 2.3°. The periodic potential is
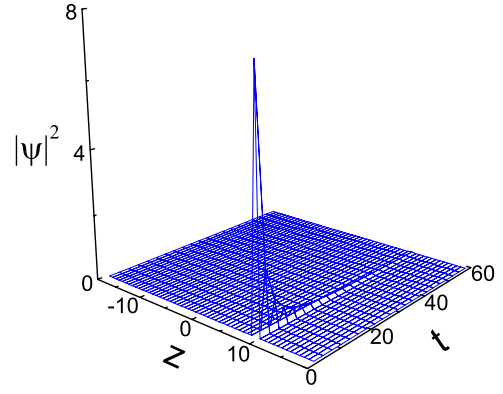

FIG. 2. (Color online). The space-time evolution of the density of the condensates in the first band gap. The Bloch wave is chosen as $u_{01}(z) = ce_1 + se_1$. The parameters used are the lattice depth $V_0 = 7.9$, interatomic interaction strength $Q' = 9 \times 10^{-3}$, the lattice spacing $D = 0.33$, the radial radius $r = 0.01$, and the chemical potential $\mu = 1.12$. All parameters are in dimensionless units.

$V = E_0 \sin^2(\pi Z/d)$ where $E_0 = 0.70 E_{rec}$ and $d = \lambda_L/2$ are the lattice depth and periodicity, respectively. Accordingly, the time and space units correspond to 0.2 ms and 3 μm, respectively. These units remain valid for other values of N, as one may vary V_0 accordingly; in this case, other quantities, such as D, also change. Based on these proposed, we obtain the dimensionless parameters $D \approx 0.33$, $Q' \approx 9 \times 10^{-3}$, and $V_0 \approx 7.9$.

As is discussed above, the nonlinear Bloch waves in the nth band gap can be given by the linear superposition of ce_n and se_n under the case of weak nonlinearity. On the basis of the fact that the coefficients of periodic Mathieu's functions depend on eigenvalue q [33] (i.e., V_0 in our notation), we presuppose that the Mathieu's functions are $ce_1 = \Sigma_{k=0}^{1000} V_0 \cos(k\eta)$ and $se_1 = \Sigma_{k=0}^{1000} V_0 \sin(k\eta)$ in the following calculation.

First, we choose a linear superposition form of $u_{01}(z) = ce_1 + se_1$ as the nonlinear Bloch wave in the first band gap. The time evolution of the density distribution of the condensates in this case is plotted in Fig. 2. We see that the peak of wave packets decreases exponentially with time and eventually vanishes. Thus the state is always unstable and is called the subfundamental soliton in Ref. [24]. Such a soliton with a very small initial total number of atoms loses a part of the atoms with as time goes on, so it is unstable (refer to Ref. [24]).

Secondly, we choose $u_{01}(z) = ce_1 + i\,se_1$, which satisfies the stable condition of soliton formation, as the nonlinear Bloch wave in the first band gap. Figure 3 shows the space-time evolution of the density the condensates in first band gap. A strong peak appears in the condensate with a dimensionless lengths of 12.6 (about 38 lattice sites), and maintains its shape and magnitude. It implies the existence of a bright gap soliton. As time goes on, the bright gap soliton is pinned in the optical lattice without both attenuation and change in shape. This behavior indicates that it is a spatially localized bright gap soliton, which is arisen from the interplay between the tunneling of periodical potential and nonlinear interaction of the system. Moreover, the width of the peak in
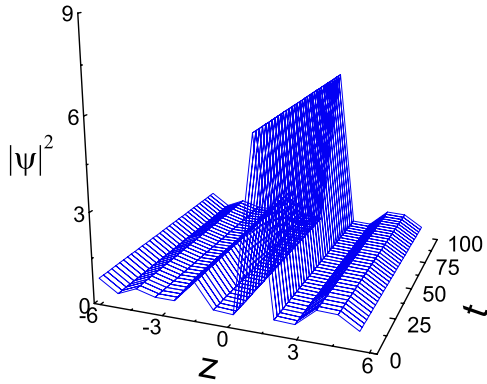
FIG. 3. (Color online) The space-time evolution of the density of the condensate with 12.6 dimensionless lengths (about 38 lattice sites), which corresponds to about 38 μm in real space. The Bloch wave is chosen as $u_{01}(z) = ce_1 + i\, se_1$. Other parameters used are the same as in Fig. 2

the $z-t$ plane is found to be a dimensionless length with 2.0, i.e., ≈ 6 μm in real space. The value is in good agreement with that of the experiment observed by Eiermann *et al.* [23]. The agreement illustrates that our method can describe the dynamics of BEC trapped in an optical lattice very well. The type of bright gap solitons are called fundamental solitons in Ref. [24]. Similar phenomena can also be obtained inside the other band gap.

From the results discussed above, the solitons residing in the band gaps are the fundamental or subfundamental solitons depending on their position in the band gap whether the stable condition of soliton formation can be satisfied or not.

In real experiment, the 1D optical lattice is created from one pair of counterpropagating laser beams, and the lattice depth depends on the peak intensity of the two identical counterpropagating laser beams. That is to say, the lattice depth can be adjusted by varying the intensity of the counterpropagating laser beams. We here depict how the lattice depth influences the fundamental soliton in Fig. 4 (with all the rest of the system parameters fixed). From solid line ($V_0 = 7.9$) and dashed line ($V_0 = 10$), one sees the amplitude of the fundamental soliton increasing with the increasing of the lattice depth. Due to both wave packets containing the same total number of atoms but the bosons in deeper well are captured more tightly, the tunneling probability varies smaller [19,37]. To balance the same nonlinear effect of the system, the tunneling rate of bosons in deeper well becomes much larger to achieve the same dispersion effect, which results in the amplitude of the fundamental soliton increasing. Therefore, the amplitude of the localized gap soliton increases with the increasing the intensity of the counterpropagating lasers beams in the experiments.

Subsequently, we observe the soliton characteristics in a longer condensate. Our numerical calculations are performed for the condensate cloud in the ground state extending over 35 dimensionless lengths (about 106 lattice sites), which corresponds to 105 μm in real space. The condensate cloud contains about 2.5×10^3 atoms under the consideration that the atomic density keeps unchanged. Figure 5 shows the space-time evolution of the density of the condensates in this
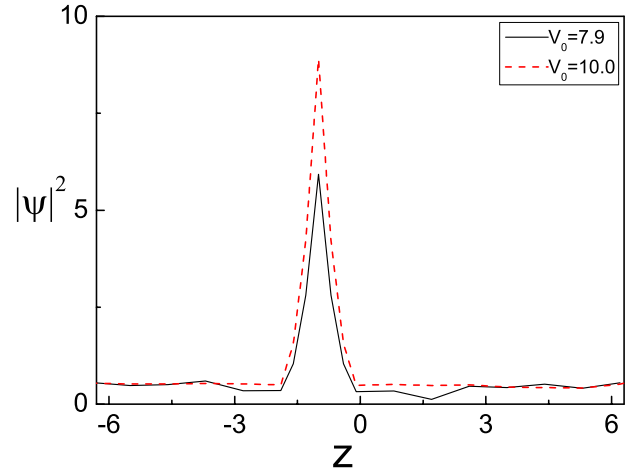

FIG. 4. (Color online) The distribution of the density of the condensates with different lattice depth at $t = 1$, where the dimensional parameter $V_0 = 7.9$ corresponds to the lattice depth in the experiment [23]. Other parameters used are the same as in Fig. 2.

case. It is shown that there exhibits a localized gap soliton train consisting of several fundamental solitons in the condensate. Similarly to the property of a single fundamental soliton, the solitonlike wave packets in the train are immobile (i.e., have zero group velocity). In reality, the condensate is loaded into an optical lattice from a crossed optical dipole trap [23], which results in an initial state of a finite extent. A BEC wave packet centered around a particular quasimomentum in a given band is created by ramping up of a static lattice with subsequent linear acceleration to a given velocity [23]. In order to observe a localized gap soliton train, we may propose experimental protocols according to the experimental observation of a single fundamental soliton [23]. First, the atoms are initially precooled in a magnetic time-orbiting potential trap using the standard technique of forced evaporation leading to a phase space density of ~ 0.03. Subsequently, the atomic ensemble is adiabatically transferred into a crossed light beam dipole trap, where further forced evaporation is achieved by lowering the light intensity in the trapping light beams. With this approach, one can generate
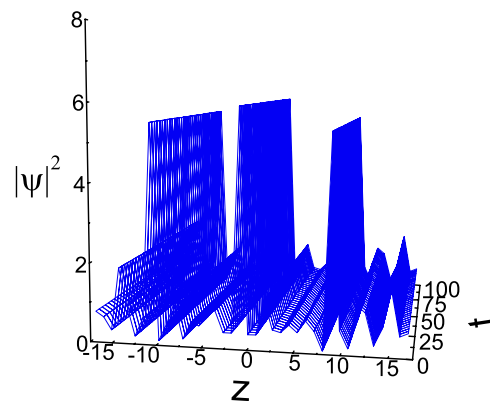

FIG. 5. (Color online) The space-time evolution of the density of the condensate with 35 dimensionless lengths (about 106 lattice sites), which corresponds to 105 μm in real space. Other parameters used are the same as Fig. 2.
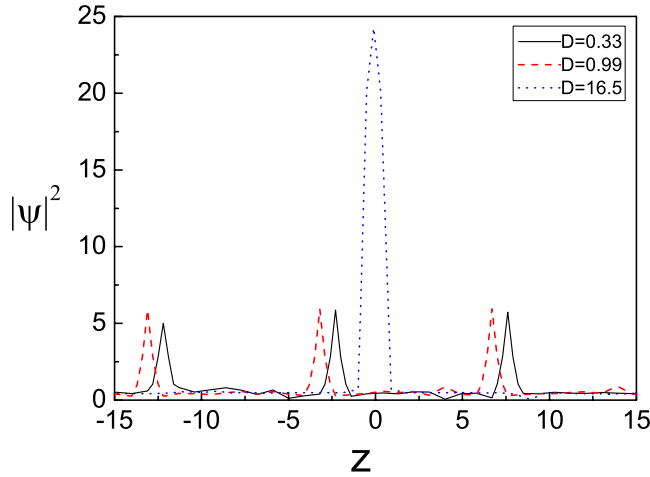
FIG. 6. (Color online) The distribution of the density of the condensates with different lattice spacing D at $t=1$, where the dimensional parameter $D=0.33$ corresponds to the lattice spacing in the experiment [23]. Other parameters used are the same as Fig. 2.

pure condensates with typically 9×10^4 atoms. By further lowering the light intensity, one can reliably produce coherent wave packets of 9000 atoms. For this atom number no gap solitons have been observed. Therefore, one removes atoms by Bragg scattering. This method splits the condensate coherently leaving an initial wave packet with 2.5×10^3 atoms at rest. Then, the wave packet centered on a particular position in a given band gap (which satisfies the stable condition of soliton formation) is created by switching off one dipole trap beam from a crossed optical dipole trap, releasing the atomic ensemble into 1D horizontal waveguide with transverse and longitudinal trapping frequencies $\omega_\perp = 2\pi \times 85$ Hz, and $\omega_\parallel = 2\pi \times 0.5$ Hz, and then accelerating the periodic potential to the recoil velocity $v_r = h/m\lambda$. This is done by introducing an increasing frequency difference between the two laser beams, creating the optical lattice. The acceleration is adiabatic, which results in an initial state of an about 105 μm extent. In view of the fact that the tunneling rate of about 900 atoms extending the length of 38 μm (in our above simulation) can balance its nonlinear energy, such a system generates a fundamental soliton. With both the length of condensate and the total number of atoms increase, the wave packet exhibits violent dynamics. During this evolution the wave packet containing 2.5×10^3 atoms is separated from the surrounding atomic cloud into several BEC wave packets, so the periodic structure of a train of the localized wave packets emerges. Such a structure represents a train consisting of several fundamental solitons, which is supported by the combined action of the repulsive nonlinearity and anomalous diffraction caused by intersite tunneling in the band gaps [16,18,38].

Finally, we study how the lattice spacing influences the fundamental soliton or soliton trains as shown in Fig. 6. In practice the variation of lattice spacing is easy to control by adjusting the angle between two counterpropagating laser beams. From solid line ($D=0.33$) and dashed line ($D=0.99$), we find that when there exists a slight difference of lattice spacing, the pinning position and the amplitude of

each fundamental soliton have little change in keeping the distance between adjacent solitons unvaried. It illuminates that the condensate cloud is separated into three wave packets for both $D=0.33$ and $D=0.99$. When the lattice spacing D varies from 0.33 to 0.99, the condensate from 91 decreases to 30 wells. Owing to the center position of each wave packet floating, the pinning position of the fundamental soliton are set to move. And each BEC the wave packet still forms a localized gap soliton, which comes from the balance between the nonlinearity and atom dispersion caused by intersite tunneling. However, when the lattice spacing D varies from 0.33 to 0.99, the number of atoms in a well increases from 28 to 83. For the same length condensate, the tunneling between adjacent well varies easier with the increasing of the atomic number confined in a well. To balance the same nonlinear energy of the system, bosons gathering around several wells vary easier, which results in the amplitude of each localized soliton having an increasing trend. When lattice spacing varies much larger [see dotted line $D=16.5$ in Fig. 6], one find that there appears only a fundamental soliton in the entire condensate with about 30 dimensionless lengths. The main reason is that the condensate in this case only contains about two wells. The tunneling of bosons in adjacent lattice achieves the dispersion effect to balance the nonlinear energy of the system, so there exhibits only a fundamental soliton in this case.

From the results discussed above, we can conclude that the condensate generating a single fundamental soliton or a localized gap soliton train consisting of several fundamental solitons can be controlled by adjusting the length of condensate or (and) the lattice spacing. Our theoretical results reported here is important in understanding the fundamental soliton physics of BEC in the future.

V. CONCLUSION

In summary, we develop the multiple scale method to study the linear and nonlinear solitary excitations for 1D BEC confined in an optical lattice. After averaging over the transverse variable, a hydrodynamical model of the amplitude and phase is derived. In the linear case, the Bloch wave in the nth energy band is the linear superposition of the Mathieu's functions ce_{n-1} and se_n, and the Bloch wave in the nth band gap is the linear superposition of ce_n and se_n. In addition, we find that the stable condition of soliton formation is that the Bloch wave u_0 in nth band gap satisfies $u_0 = \beta ce_n + i\beta se_n$. Under this stable condition, a linear dispersion relation and sound speed are derived. It is found that the linear dispersion relation and sound speed depend mainly on the lattice spacing.

For the nonlinear case, we derive a solution of the wave function of the condensates with weakly interatomic interaction, and discuss its stability for condensate ^{87}Rb in band gaps. It shows that there are two types of gap solitons in the band gaps. One is the fundamental soliton, which is always stable and pins a fixed position; the other is the subfundamental soliton which is always unstable and decays gradually due to losing a part of its atoms. Only when the Bloch

wave in the band gaps satisfies the stable condition, the condensates exhibit the fundamental solitons, otherwise there appears the subfundamental solitons. Furthermore, the pinning position and the amplitude of the fundamental solitons in the lattice can be controlled by varying the lattice depth and spacing. We also propose an experimental protocol to observe a localized gap soliton train consisting of several fundamental solitons for BEC trapped in an optical lattice in future experiment.

[1] M. Barrett, J. Sauer, and M. S. Chapman, Phys. Rev. Lett. **87**, 010404 (2001).

[2] C. Orzel, A. K. Tuchman, M. L. Fensclau, M. Yasuda, and M. A. Kasevich, Science **291**, 2386 (2001).

[3] F. S. Cataliotti, S. Burger, C. Fort, P. Maddaloni, F. Minardi, A. Trombettoni, A. Smerzi, and M. Inguscio, Science **293**, 843 (2001).

[4] M. Greiner, O. Mandel, T. Esslinger, T. W. Hansch, and I. Bloch, Nature (London) **415**, 39 (2002).

[5] A. S. Desyatnikov, E. A. Ostrovskaya, Y. S. Kivshar, and C. Denz, Phys. Rev. Lett. **91**, 153902 (2003); G. P. Berman, F. Borgonovi, F. M. Izrailev, and A. Smerzi, *ibid.* **92**, 030404 (2004); J. Yang, I. Makasyuk, P. G. Kevrekidis, H. Martin, B. A. Malomed, D. J. Frantzeskakis, and Z. G. Chen, *ibid.* **94**, 113902 (2005).

[6] B. B. Baizakov, B. A. Malomed, and M. Salerno, Phys. Rev. E **74**, 066615 (2006); H. Sakaguchi and B. A. Malomed, *ibid.* **72**, 046610 (2005); B. Baizakov, G. Filatrella, B. Malomed, and M. Salerno, *ibid.* **71**, 036619 (2005).

[7] K. Staliunas, R. Herrero, and G. J. de Valcarcel, Phys. Rev. E **73**, 065603(R) (2006); G. X. Huang, L. Deng, and C. Hang, *ibid.* **72**, 036621 (2005); D. E. Pelinovsky, D. J. Frantzeskakis, and P. G. Kevrekidis, *ibid.* **72**, 016615 (2005).

[8] E. Kengne and W. M. Liu, Phys. Rev. E **73**, 026603 (2006); L. Li, B. A. Malomed, D. Mihalache, and W. M. Liu, *ibid.* **73**, 066610 (2006); V. A. Brazhnyi and V. V. Konotop, *ibid.* **72**, 026616 (2005).

[9] G. Theocharis, D. J. Frantzeskakis, R. Carretero-Gonzalez, P. G. Kevrekidis, and B. A. Malomed, Phys. Rev. E **71**, 017602 (2005); D. E. Pelinovsky, A. A. Sukhorukov, and Y. S. Kivshar, *ibid.* **70**, 036618 (2004); B. A. Malomed, T. Mayteevarunyoo, E. A. Ostrovskaya, and Y. S. Kivshar, *ibid.* **71**, 056616 (2005).

[10] E. P. Fitrakis, P. G. Kevrekidis, H. Susanto, and D. J. Frantzeskakis, Phys. Rev. E **75**, 066608 (2007); D. L. Machacek, E. A. Foreman, Q. E. Hoq, P. G. Kevrekidis, A. Saxena, D. J. Frantzeskakis, and A. R. Bishop, *ibid.* **74**, 036602 (2006).

[11] Z. X. Liang, Z. D. Zhang, and W. M. Liu, Phys. Rev. Lett. **94**, 050402 (2005); A. C. Ji, X. C. Xie, and W. M. Liu, *ibid.* **99**, 183602 (2007).

[12] A. Trombettoni and A. Smerzi, Phys. Rev. Lett. **86**, 2353 (2001); A. Smerzi and A. Trombettoni, Phys. Rev. A **68**, 023613 (2003).

[13] F. K. Abdullaev, B. B. Baizakov, S. A. Darmanyan, V. V. Konotop, and M. Salerno, Phys. Rev. A **64**, 043606 (2001).

[14] O. Zobay, S. Pötting, P. Meystre, and E. M. Wright, Phys. Rev.

A **59**, 643 (1999).

[15] G. L. Alfimov, P. G. Kevrekidis, V. V. Konotop, and M. Salerno, Phys. Rev. E **66**, 046608 (2002).

[16] H. Pu, L. O. Baksmaty, W. Zhang, N. P. Bigelow, and P. Meystre, Phys. Rev. A **67**, 043605 (2003).

[17] N. K. Efremidis and D. N. Christodoulides, Phys. Rev. A **67**, 063608 (2003).

[18] V. V. Konotop and M. Salerno, Phys. Rev. A **65**, 021602(R) (2002).

[19] O. Morsch and M. Oberthaler, Rev. Mod. Phys. **78**, 179 (2006).

[20] K. M. Hilligsoe, M. K. Oberthaler, and K. P. Marzlin, Phys. Rev. A **66**, 063605 (2002); V. Ahufinger, A. Sanpera, P. Pedri, L. Santos, and M. Lewenstein, *ibid.* **69**, 053604 (2004).

[21] S. Pötting, M. Cramer, and P. Meystre, Phys. Rev. A **64**, 063613 (2001); H. A. Cruz, V. A. Brazhnyi, V. V. Konotop, G. L. Alfimov, and M. Salerno, *ibid.* **76**, 013603 (2007).

[22] P. J. Y. Louis, E. A. Ostrovskaya, C. M. Savage, and Y. S. Kivshar, Phys. Rev. A **67**, 013602 (2003).

[23] B. Eiermann, T. Anker, M. Albiez, M. Taglieber, P. Treutlein, K. P. Marzlin, and M. K. Oberthaler, Phys. Rev. Lett. **92**, 230401 (2004).

[24] T. Mayteevarunyoo and B. A. Malomed, Phys. Rev. A **74**, 033616 (2006).

[25] E. A. Ostrovskaya and Y. S. Kivshar, Phys. Rev. Lett. **90**, 160407 (2003).

[26] M. Matuszewski, W. Krolikowski, M. Trippenbach, and Y. S. Kivshar, Phys. Rev. A **73**, 063621 (2006).

[27] P. G. Kevrekidis, D. J. Frantzeskakis, R. Carretero-Gonzalez, B. A. Malomed, G. Herring, and A. R. Bishop, Phys. Rev. A **71**, 023614 (2005).

[28] C. Menotti, M. Kraemer, A. Smerzi, L. Pitaevskii, and S. Stringari, Phys. Rev. A **70**, 023609 (2004).

[29] T. Busch and J. R. Anglin, Phys. Rev. Lett. **84**, 2298 (2000).

[30] G. X. Huang, M. G. Velarde, and V. A. Makarov, Phys. Rev. A **64**, 013617 (2001); G. X. Huang, J. Szeftel, and S. H. Zhu, *ibid.* **65**, 053605 (2002).

[31] A. E. Muryshev, H. B. vanLindenvandenHeuvell, and G. V. Shlayapnikov, Phys. Rev. A **60**, R2665 (1999).

[32] D. W. Jordan and P. Smith, *Nonlinear Ordinary Differential Equations* (Clarendon Press, Oxford, 1977).

[33] I. S. Gradshteyn and I. M. Rhyzhik, *Table of Integrals, Series, and Products*, 4th ed. (Academic, New York, 1980), p. 991, Sec. 8.60.

[34] M. Cristiani, O. Morsch, J. H. Muller, D. Ciampini, and E. Arimondo, Phys. Rev. A **65**, 063612 (2002); O. Morsch, M.

Cristiani, J. H. Muller, D. Ciampini, and E. Arimondo, *ibid.* **66**, 021601(R) (2002).

[35] P. G. Kevrekidis, R. Carretero-Gonzalez, G. Theocharis, D. J. Frantzeskakis, and B. A. Malomed, Phys. Rev. A **68**, 035602 (2003).

[36] M. R. Andrews, D. M. Kurn, H. J. Miesner, D. S. Durfee, C. G. Townsend, S. Inouye, and W. Ketterle, Phys. Rev. Lett. **79**, 553 (1997); **80**, 2967 (1998).

[37] Q. Niu, X. G. Zhao, G. A. Georgakis, and M. G. Raizen, Phys. Rev. Lett. **76**, 4504 (1996); W. M. Liu, W. B. Fan, W. M. Zheng, J. Q. Liang, and S. T. Chui, *ibid.* **88**, 170408 (2002).

[38] B. J. Dabrowska, E. A. Ostrovskaya, and Y. S. Kivshar, Phys. Rev. A **73**, 033603 (2006).